Silica Coated Plasmonic Nanobone-based Tags for Safe Bioimaging

Aleksei N. Smirnov[a], Vasilisa O. Svinko[b], Aleksei S. Strelnikov[c], Alisa I. Shevchuk[d], Anna V. Volkova[e] and Elena V. Solovyeva[f]
Chemistry Institute, Saint-Petersburg State University, 26 Universitetsky pr., Peterhof, Saint-Petersburg, Russia

Keywords: Gold, Nanobone, Bioimaging, Tag, Fluorescence, SERS, Cyanine, Stober.

Abstract: Fluorescence tomography is a hopeful medical imaging technique. However, this method has restrictions consisting in absorbance and scattering of optical signal by tissue. The present research is devoted to overcome these challenges utilising plasmonic nanoparticles. A new type of gold nanoparticles was synthesized, having a bone-like shape which provides the maximum of unimodal absorption band just in the middle of the biological tissues transparency range (600-800 nm). The nanobones were further modified with cyanine 5.5 and 7 fluorophores by electrostatic immobilization and coated by silica shell via two different techniques to instill biocompatibility. Resulting nanoparticles were characterised by dynamic light scattering, transmission electron microscopy, fluorescent and Raman spectroscopy. It is shown that a thickness of silica shell may be tuned precisely and that the nanoparticles may also be coated directly using mercaptopropyltrimethxysilane. The registered surface-enhanced Raman scattering and fluorescent signals depend on a position of cyanine dye in nanoparticle shell. Intensive fluorescent signal from the nanoparticles covered with silicon dioxide using mercaptopropyltrimethxysilane proved an incorporation of cyanines into shell during its growth.

1 INTRODUCTION

Optical labels basing on a fluorophore modified by specific antibody began to be used in medical practice in the last decade and have already proven their effectiveness (Benitez, Zanca, Ma, Cavenee, & Furnari, 2018). Meanwhile many techniques have been developed that make it possible to synthesize plasmonic nanoparticles (NPs) that amplify an optical signal by several orders of magnitude (some works deal with determination of single molecules) (Le Ru et al., 2011; Ren, Liu, Guo, & Wang, 2011; Sharma, Frontiera, Henry, Ringe, & Van Duyne, 2012; Solovyeva, Ubyivovk, & Denisova, 2018). The literature provides the examples of amplification of Raman scattering or fluorescence by 10^4-10^8 times (Amendola, Pilot, Frasconi, Maragò, & Iatì, 2017; Phan-Quang et al., 2019).

Light passing through biological tissues is scattered and absorbed, so the currently used methods of fluorescence tomography and photodynamic therapy are used only for superficial tissues (Castano, Mroz, & Hamblin, 2006; Lapchenko, 2015; Wang, Wang, Luo, & Yang, 2015). Thus, one of the main tasks is to "adjust" the range of optical activity of the labels in the region of transparency of biological tissues in order to visualize objects located in tissue deeper without interference, or to carry out laboratory analysis with a higher degree of selectivity in the absence of a signal from biological matrix. This range is the red border of the visible spectrum, named the “region of transparency” is between 600 and 800 nm.

The use of chromophores, is possible both, as fluorescent and as Raman labels. When the absorption ranges of label and plasmonic NP coincides, the conditions of surface-enhanced Raman scattering and fluorescence may be achieved. The chromophores cyanine 5.5 and cyanine 7 were

[a] https://orcid.org/0000-0003-0045-9631
[b] https://orcid.org/0000-0001-5246-4999
[c] https://orcid.org/0000-0002-8193-7457
[d] https://orcid.org/0000-0002-7968-4710
[e] https://orcid.org/0000-0001-8650-8312
[f] https://orcid.org/0000-0002-5046-3543

Smirnov, A., Svinko, V., Strelnikov, A., Shevchuk, A., Volkova, A. and Solovyeva, E.
Silica Coated Plasmonic Nanobone-based Tags for Safe Bioimaging.
DOI: 10.5220/0010997700003121
In *Proceedings of the 10th International Conference on Photonics, Optics and Laser Technology (PHOTOPTICS 2022)*, pages 179-186
ISBN: 978-989-758-554-8; ISSN: 2184-4364

already investigated as fluorescent labels incorporated in silica NPs (Lane, Qian, & Nie, 2015). The resulting tags showed high stability in saline as well as in real blood samples.

Spherical particles were historically obtained firstly, however, they do not possess some unique properties inherent for anisotropic NPs. Numerous synthetic techniques have been proposed for gold NPs and the quality of various forms. In particular, nanostars make it possible to achieve the conditions of "hot spots" within a single NP, when a chromophore molecule is adsorbed between two rays of a star, nanocages allow themselves to be used as a container for other objects, and nanorods and their various modifications make it possible to adjust the position of the plasmon resonance peak in a wide range (Huang et al., 2019; G. W. Kim & Ha, 2018; Maysinger, Moquin, Choi, Kodiha, & Stochaj, 2018; Panda, Chakraborti, & Basu, 2018). The last type of gold nanoparticles of the rod-shaped family and their derivatives, such as bipyramids, which have already proven themselves as plasmon substrates that provide high signal amplification and the ability to use for bioanalytical and medical purposes (Sahu et al., 2021; Uchehara, Kirk, Trifiro, Paliouras, & Mohammadyousef, 2019).

On the basis of nanorods, multimodal SERS-tags were proposed by the scientific group of Alastair W. Work, containing dyes of the cyanine class as Raman tags, covering the optical range from 514 to 1064 nm. Since the nanorods themselves have an absorption peak at 800 nm, the most intense scattering was recorded with excitation at 785 nm. The chromophores cyanine 5.5 and cyanine 7 were investigated as fluorescent labels - modifiers of whole silicon oxide nanoparticles (Biffi et al., 2016). The resulting particles showed high stability in saline solution as well as in real blood samples.

In order for the obtained labels to be, firstly, stable, and secondly, biologically neutral, it is necessary to cover with a shell. Gold nanoparticles coated with silicon oxide have shown the possibility of a real analytical application e.g. for an analysis of oranges for pesticide content by the SERS method (Feng Li et al., n.d.). The silica surface can be further functionalized to attach vectors or fluorophores.

Polyallylamine hydrochloride can be used in combination with an anionic polyelectrolyte, such as polystyrene sulfonate, to form layer-by-layer adsorbed films of negatively and positively charged polymer (Bodelón et al., 2015). Thus-obtained materials have many biomedical applications and can be further coated with silica dioxide shell (J. Kim et al., 2015).

The aim of this work is to develop nanomarkers with a plasmon resonance peak position in the 600-800 nm range, suitable for multimodal SERS and fluorescent optical analytical purposes and coated with silica to obtain stability in a biological matrix and biocompatibility. The long-term research target is the development of nanocomposite labels for *in vitro* and *in vivo* applications. These labels can be used for sensitive tumor localization, metabolic studies, pharmacokinetics of substances, visualization of organ and tumor structures, detection of ultra-low concentrations of substances in the transparency of biological tissues, as well as plasmon tomography guided surgical manipulations. Such labels, even at very low concentrations, will give a signal that is observed through the thickness of biological tissue.

2 MATERIALS

2.1 Chemicals

Cetyltrimethylammonium bromide (CTAB) (Sigma-Aldrich, 95%), hydrogen tetrachloroaurate ($HAuCl_4$) (Alfa Aesar, 99%), cyanine 7 amine (Lumiprobe, 95%), cyanine 5.5 amine (Lumiprobe, 95%), sodium borohydride ($NaBH_4$) (Sigma-Aldrich, 99%), ascorbic acid (Sigma-Aldrich, 99%), silver nitrate ($AgNO_3$) (Sigma-Aldrich, 99%), polystyrene sulfonate (PSS) (Sigma-Aldrich, 95%), poly(allylamine hydrochloride) (PAH) (Sigma-Aldrich, 95%), polyvinylpyrrolidone (PVP) (Sigma-Aldrich, 95%), mercaptopropyltrimethxysilane (MPTMS) (Sigma-Aldrich, 97%), triethoxysilane (TEOS) (Sigma-Aldrich, 99%). All reagents were used without additional purification. All glass dishes were washed with aqua regia and rinsed with deionized water prior to the use.

2.2 Synthesis of Gold Nanobones Core

The synthesis of gold bone-like nanoparticles based on the procedure described for gold nanorods and differed in the ratio of reagents used and reaction conditions (Pastoriza-Santos, Pérez-Juste, & Liz-Marzán, 2006). The general synthesis procedure and reagents quantities for 400 ml of final colloid are described below.

Seed solution: 5 ml of 0.2M CTAB was mixed 5 ml of 0.1 mM $HAuCl_4$, then 0.6 ml of ice-cold $NaBH_4$ was added. The solution goes from pink to creamy yellow.

Growth solution: 200 ml of 0.2 M CTAB solution was mixed with 10 ml of 10 mM $AgNO_3$ under

vigorous stirring, then 200 ml of 1 mM $HAuCl_4$ was added. Subsequently 2.8 ml of ascorbic acid and 0.552 ml of Seed solution were added simultaneously. The solution should be discolored after that. The reaction was stirred for 48 in dark place at 25º C. The final colloid is dark blue.

The resulting colloid was centrifuged twice: the first time at 10000 rpm and the second time at 8500 rpm in 50 ml tubes to remove excess CTAB. The colloid was then resuspended in deionized water to the desired volume. The resulting colloid was sonicated for 30 minutes before being used as such after all subsequent coating steps.

2.3 Silica Coating over Polyelectrolyte Layers

The scheme of coating with polyelectrolytes layers was created and optimized experimentally on the basis of Stober method (Christina Graf, Dirk L. J. Vossen, Arnout Imhof, & Alfons van Blaaderen, 2003; Pastoriza-Santos et al., 2006). 100 ml of the purified colloid was added dropwise with stirring to 100 ml of a solution containing 2 g/L PSS, 6 mM NaCl, and stirring was left until the next day. The resulting 200 ml was purified by centrifugation at 8500 rpm to remove excess PSS and resuspended in H_2O. The PAH and PVP layers were introduced similarly as 2 g/L and 4 g/L solutions, followed by centrifugation at 7500 and 6500 rpm, respectively. The PVP coated colloid was resuspended to 5 ml before being coated with silica.

Cyanines were added dropwise in the form of 10^{-4} M solutions at the ratio of 1:9 volumes of the dye to the colloid and left under vigorous stirring for 2 hours before coating with polyelectrolytes PSS (2a and 2b), PAH (3a and 3b) and PVP (4a and 4b) according to the procedure described above (Fig. 2), where the index "a" corresponds to nanoparticles modified with cyanine 7 amines 5.5, and the index "b". Cyanines were added dropwise at any stage in the form of 10^{-4} M solutions in the form of 1:9 volumes of colloid and left under vigorous stirring for 2 hours.

Silica coating: 5 ml of concentrated PVP coated hydrosol was poured into 8 ml of isopropanol (i-Pr). The resulting mixtures were divided into 5 parts by 3 ml of colloid. With magnetic stirring, 2.84 ml of 1.27% NH_3/i-Pr (prepared by mixing 1.01 ml of 25% aqueous ammonia and 18.98 ml of i-Pr) was added. TEOS solutions prepared from a stock 0.97% solution in isopropanol were added according to the following table (Table 1).

The numbers, which are given in Table 1, correspond to the numbers of the samples given in the TEM photographs (Fig. 4). The linear step of the mean radius of the shell should be in inverse cubic dependence on the TEOS concentration (Table 1).

Table 1: TEOS concentrations used for coating PVP-stabilized nanoparticles with silicon oxide. The second column gives the cubic root of this concentration to show the calculated linearity of the shell radius step. The total volume of TEOS added in all cases was equal to 400 μL; therefore, in the case of lower concentrations, the volume was adjusted with isopropanol.

№	TEOS content, v/v, %	^1/3, calc. relative radius	0.97% TEOS/iPr stock	iPr
5	0.00101	1.84	13	387
4	0.00372	2.84	46	354
3	0.00922	3.85	114	286
2	0.01844	4.85	228	172
1	0.03234	5.85	400	0

2.4 Silica Coating via Covalent Linker

A solution of MPTMS in isopropanol with concentration of 10^{-4} M was added to unmodified nanobones in the ratio of 1:10 after their purification from excess CTAB. The mixture was stirred for 24 hours then unreacted MPTMS was removed by centrifugation. The colloid was resuspended in a volume of isopropanol 20 times less than the volume of the original colloid. Next, the particles were coated with silica by a technique similar to the coating by TEOS using the concentration of 0.032 vol. % and left stirring in a dark place overnight.

2.5 Methods

The UV-Vis absorption spectra of NP solutions were recorded in the range of 190-1100 nm on a spectrometer UV-1800 (Shimadzu) in quartz cells with an optical path length of 10 mm.

Transmission electron microscopy (TEM) images of gold nanoparticles were obtained with a Zeiss Libra 200FE microscope at an accelerating voltage of 200 kV. In order to prepare samples for TEM measurements, 10 μl of the silver nanoparticle solutions were drop casted on top of carbon films and air dried.

The dynamic light scattering (DLS) study was performed on a Zetasizer Nano ZS (Malvern Instruments Ltd.) with 633 nm laser line. The refractive index value of 0.27 was used for gold in

Smoluchowski equation. The viscosity of solvent was set as 0.887 Pa for water and refractive index was set as 1.33.

Surface-enhanced Raman scattering (SERS) spectra were acquired on a SENTERRA express Raman spectrometer (Bruker) exciting by 785 nm laser line with output power of 40 mW. The emission spectra were recorded on a LabRam HR 800 spectrometer (Horiba Jobin Yvon) with excitation by 633 nm line. The fluorescence spectra in scanning regime were recorded on a spectrofluorophotometer RF-5301 PC (Shimadzu).

3 RESULTS ANS DISCUSSION

3.1 Morphology and Surface Properties

According to the TEM micrograph (inset in Fig. 1), the obtained gold nanoparticles have an unusual shape of nanobones. These nanobones have the distinct absorption band at 700 nm, covering the spectral range from 600 nm to 800 - i.e., perfectly matching the biological tissue transparency window (Fig. 1).

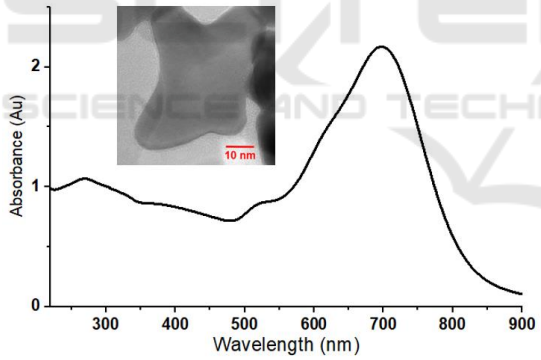

Figure 1: The UV-Vis absorption spectrum and TEM image of the obtained gold nanobones.

Moreover, these particles have almost invisible shoulder near 530 nm. In many methods for the synthesis of rod-like and related nanoparticles, spherical particles with absorption in the 530 nm region also form as a byproduct, that is undesirable (Pastoriza-Santos et al., 2006). At the same time, their separation is a rather complicated, resource-intensive and ineffective process. The plasmon band of synthesized nanobones is of high intensity, but at the same time is rather diffuse, which allows measurements at excitation by both, 632.8 nm and 785 nm laser lines. The synthesis is reproducible using reagents from different sources.

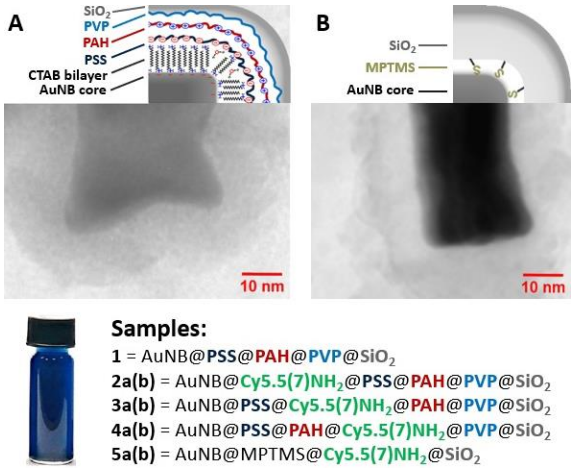

Figure 2: Schematic representation of polyelectrolyte layer-by-layer coating of CTAB-stabilized gold nanoparticles with electrostatic encapsulation of chromophore schematically overlapped with corresponding TEM images. A. B. Gold nanobone core, coated with silica dioxide via MPTMS. Brackets represent one of the two cyanines. For example, the sample 2a corresponds to the nanotag with incorporated cyanine 5.5, while the sample 2b contains cyanine 7. Bottom left –photograph of nanobones solution prior to coating.

Fig. 2 shows the TEM micrographs of nanoparticles coated with a silicon oxide shell using two synthetic procedures that fundamentally differ in the method of creation of a surface affine to the incipient silicon oxide shell. The schematic representation of a cut of nanoparticles is intended to simplify the perception of their structure.

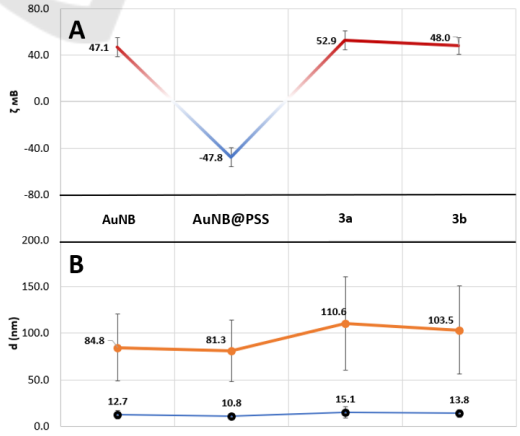

Figure 3: A. Zeta potential curve, which represents a recharge of gold NB surface after PSS and PAH deposition and the final values for the samples 3a and 3b. B. The hydrodynamic diameters of these nanoparticles.

Meanwhile, a study of nanoparticles size using the dynamic light scattering method showed the presence of two peaks (Fig. 3). The peak corresponding to the diameter value of 85 nm correlates well with those of the TEM micrograph (Fig. 1, Fig. 3), increase of this value to 100-110 nm correlates with the images of silica-covered nanoparticles. In contrast, the 10-15 nm peak cannot be matched with any of that sizes in the TEM images. This result is reproducible, while for other nanoparticles, such as nanorods, this phenomenon was not observed.

The TEM images show a translucency of gold nanobones, that is especially noticeable in the places where the nanoparticles lie on top of each other (Fig. 1). The hypothesis is that the peak corresponding to the value around 10-15 nm is obtained when a light scatters from the side edge of particle. Thus, we can conclude that these particles are thin flat plates.

Bioanalytical applications imply a need to work with media containing large amounts of salts. Silica coating is a versatile method for stabilizing nanoparticles, preventing their degradation in various environments. Silica surface can be further functionalized to immobilize covalently various molecules, in particular delivery vectors.

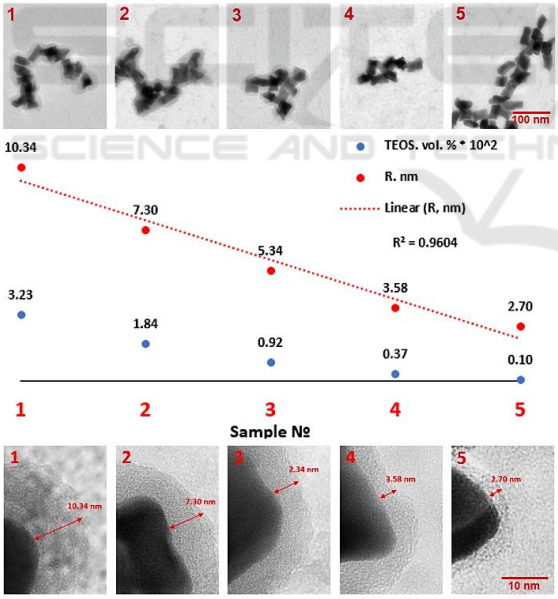

Figure 4: TEM images, representing the shell thickness of silica coated gold nanobones. The red digits indicate a sample number corresponding to the decrease in TEOS concentration. The graph displays a dependence of the shell thickness of gold nanobones on the concentration of TEOS, plotted for the corresponding nanoparticles.

When calculating the TEOS concentration for each sample, we proceeded from the assumption of inverse cubic dependence of the shell thickness from the concentration, taking into account a spherical approximation, i.e. that the concentration of surface modifier is directly proportional to the volume of sphere (Figure 4).

According to the TEM results, a linear increase in the thickness of silicon oxide shell was obtained (Figure 4). TEM micrographs may give the impression that the particles are stuck together in oxide shells. However, UV-Vis measurements indicated that these are separate particles. According to the absorption spectra of solution, the position of the plasmon resonance band does not undergo to a redshift that is should be observed during formation of dimers and agglomerates of nanoparticles. A visual inspection showed also that the solutions retain their blue color.

Particles on a TEM micrograph look like this because of the "coffee stain" effect, which appear when the solvent evaporates after the particles are deposited on copper substrates.

The second approach to coating of CTAB-stabilized gold nanobones consisted in covalent interaction of mercaptopropyl-trimethoxysilane (MPTMS) with the gold surface and subsequent coating with silica by hydrolysis of TEOS. This approach has been criticized in the literature as particles can coagulate during direct coating (Pastoriza-Santos et al., 2006).

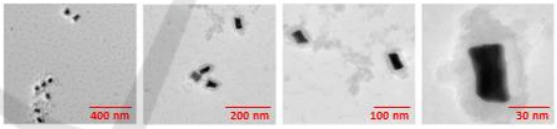

Figure 5: The TEM images of gold nanobones coated by silica through MPTMS.

It can be seen that the shell morphology of thus-synthetized nanoparticles is less uniform than in the case of shell, which was created after PVP layer (Fig. 5). Nevertheless, this approach is much more fast and easier to implement and certainly deserves further development.

3.2 Raman and Fluorescence Spectroscopy Study

Intense fluorescence spectra were obtained for both cyanine 5.5 and cyanine 7 containing nanobones. Moreover, intensity of signal depended critically on the position of fluorophore in the polymer shell (Fig. 6).

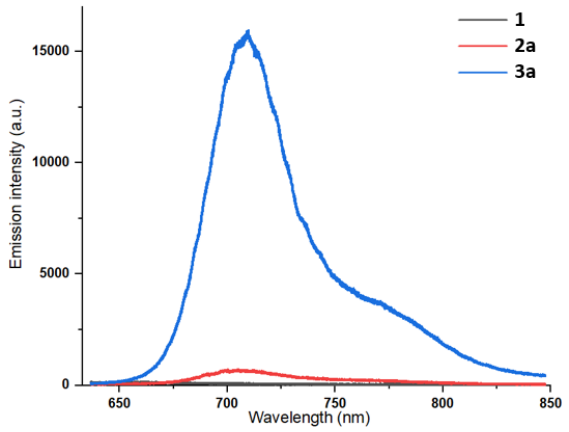

Figure 6: Comparison of emission signal of gold nanobones coated with silicon oxide and modified with cyanine 5.5 amine located in different layers (see the description of the samples indexes in Fig. 2).

The polyelectrolyte layers make it possible to move fluorophore away from the surface, interaction of which with the surface quenches the fluorescence signal. By placing cyanine 5.5 after the second polymer layer with successive layering, we were able to obtain the fluorescence signal (Fig. 6, blue curve, sample 3a). The graph (Fig. 6) shows that the emission of fluorophore upon excitation at 633 nm (red curve, sample 2a), differs slightly from the control nanoparticles, also coated by silica but without fluorophore (black curve, sample 1).

The complete fluorescence pattern of the synthesized systems is shown in Fig. 7. From this data, it can be concluded about a contribution of reabsorption. A tenfold dilution of solution of the nanoparticles coated by silicon oxide with fluorophore in the second layer led to the increase in emission intensity in red range and to change in the contour in ultraviolet range.

A similar trend was also observed for the samples that contained cyanine 5.5 amine and cyanine 7 amines in the first layer coated with silica by direct modification with MPTMS (Figs. 7B, 7C). It is curious that in this case cyanines retain their fluorescent activity in the red range and do not undergo to quenching. According to the TEM results, the shell has the thickness about 10 nm. During the coating process, fluorophore is, probably, incorporated into silicon oxide, thus, located at a sufficient distance from the surface so that fluorescence was not quenched completely.

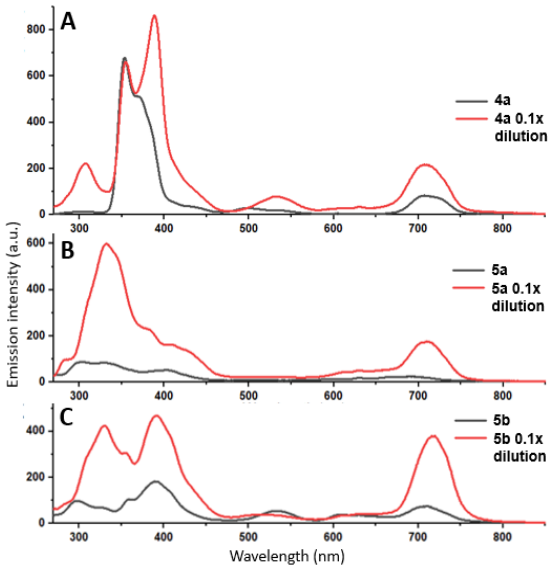

Figure 7: The fluorescence spectra recorded in scanning mode with a step of 50 nm. The scanning mode consists in a parallel shift of excitation wavelength and registration of secondary radiation and allows obtaining an overall picture of emission activity of substance which Stokes shift is equal to step value.

These spectra are also characterized by a presence of strong ultraviolet radiation, which was not observed for uncoated particles. In the case of the samples shown in Fig. 7.B and 7.C, a contribution of polyvinylpyrrolidone, known for its fluorescence in the 380-400 nm region, is likely (Song et al., 2015). It is difficult to draw unambiguous conclusions about an origin of emission registered in the range of 300-350 nm, as well as emission in the range of 350-450 nm for the samples in Fig. 7.A, because only MPTMS, TEOS and cyanine 5.5 were used in the synthesis of these samples.

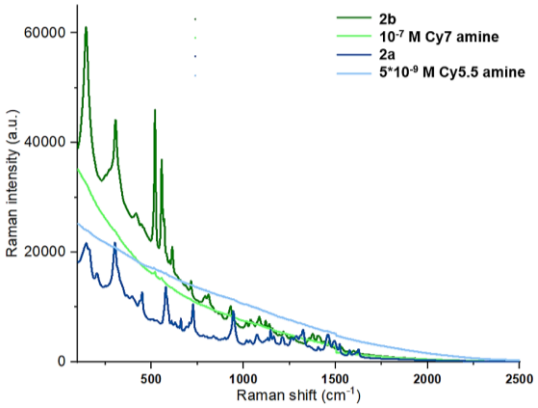

Figure 8: The SERS spectra obtained for the samples 2a and 2b at 785 nm excitation. The spectra of pure cyanines solutions are represented for comparison.

Plasmonic nanoparticles have long proven themselves as an effective tool for obtaining information in the field of fingerprints for those substances for which this is not possible by other methods due to high fluorescence and/or low solubility (Etchegoin & Ru, 2010). By irradiating the samples 2a and 2b with 785 nm laser line, it became possible to obtain the characteristic Raman spectra of cyanines 5.5 and 7 for the first time (Fig. 8). Chromophores were used in the form of positively charged cations and were added after the first layer of negatively charged polyelectrolyte. Thus, good electrostatic adsorption was ensured, and the chromophores were located close enough to the surface to observe an intense SERS signal.

4 CONCLUSIONS

Novel technique has been developed for the synthesis of bone-like gold nanoparticles with a unimodal plasmon resonance band which appears in the middle of biological tissues transparency window (600-800) and provides the opportunity to excite plasmon resonance by conventional medical lasers 632.8 and 785 nm.

The nanobones were modified using two fluorophores: cyanine 5.5 amine and cyanine 7 amine as optical reporters. The possibility of using modified nanoparticles as fluorescent and SERS labels was shown when using lasers with wavelengths of 632.8 and 785 nm, respectively. This multimodality became possible due to a change in the distance of fluorophore from the surface due to a layer-by-layer alteration of oppositely charged polyelectrolytes.

Highly characteristic surface-enhanced Raman spectra of cyanine 5.5 amine and cyanine 7 amine were obtained firstly when dye was placed between first and second polyelectrolyte layers. Fluorescence is almost completely quenched at such dye position. High intensity unstimulated fluorescence was obtained from nanotags when cyanine was placed between the second and third polyelectrolyte layers.

Nanobones with three polyelectrolyte layers were additionally coated with silicon dioxide shell according to the Stober method to ensure biocompatibility and to prevent a leaching of chromophores and polyelectrolytes into biological matrix. The relationship between the concentration of surface modifier and the thickness of resulting shell was revealed: it was possible to ensure an accurate linear increase in the shell thickness from 2.7 to 10.3 nm.

In addition, a method of coating nanobones with silicon oxide without polyelectrolytes using mercaptopropyltrimethxysilane was carried out. The mercaptopropyltrimethxysilane approach allows to perform a surface coverage in just two steps, but produces more irregular morphology. A noticeable fluorescent signal from nanoparticles coated with MPTMS indicates the incorporation of cyanine into the silica shell during its growth. Thus, such NPs are also suitable candidates for bioanalytical tags.

The results of the work confirm the prospects of transition to extended cell tests with obtained nanoparticles for the development of methods of optical diagnostics. Distinctive features of the proposed approach are the simplicity of synthesis, high optical response and biocompatibility of obtained tags.

ACKNOWLEDGEMENTS

The authors acknowledge Saint-Petersburg State University for financial support within the programme “Creation of laboratory under a young scientist leadership”. The authors would like to thank the Resource Centres of SPbU: "Optical and Laser Materials Research", "Chemical Analysis and Material Research", "Magnetic Resonance Research", "Nanotechnology".

REFERENCES

Amendola, V., Pilot, R., Frasconi, M., et al. (2017, April 20). Surface plasmon resonance in gold nanoparticles: A review. *Journal of Physics Condensed Matter*. Institute of Physics Publishing.

Benitez, J. A., Zanca, C., Ma, J., et al. (2018). Fluorescence molecular tomography for in vivo imaging of glioblastoma xenografts. *Journal of Visualized Experiments*, 2018(134).

Biffi, S., Petrizza, L., Garrovo, C., et al. (2016). Multimodal near-infrared-emitting PluS Silica nanoparticles with fluorescent, photoacoustic, and photothermal capabilities. *International Journal of Nanomedicine*, 11, 4865–4874.

Bodelón, G., Montes-García, V., Fernández-López, C., et al. (2015). Au@pNIPAM SERRS Tags for Multiplex Immunophenotyping Cellular Receptors and Imaging Tumor Cells. *Small*, 11(33), 4149–4157.

Castano, A. P., Mroz, P., & Hamblin, M. R. (2006, July). Photodynamic therapy and anti-tumour immunity. *Nature Reviews Cancer*. Nature Publishing Group.

Christina Graf, *,†,§, Dirk L. J. Vossen, †,‡, Arnout Imhof, † and, et al. (2003). A General Method To Coat Colloidal Particles with Silica.

Etchegoin, P. G., & Ru, E. C. L. (2010). Basic Electromagnetic Theory of SERS. In *Surface Enhanced Raman Spectroscopy: Analytical, Biophysical and Life Science Applications* (pp. 1–37). Weinheim, Germany: Wiley-VCH.

Feng Li, J., Fan Huang, Y., Ding, Y., et al. (n.d.). Shelled-isolated nanoparticle-enhanced Raman spectroscopy.

Huang, Y., Lin, D., Li, M., et al. (2019). Ag@Au core-shell porous nanocages with outstanding sers activity for highly sensitive SERS immunoassay. *Sensors (Switzerland)*, 19(7).

Kim, G. W., & Ha, J. W. (2018). Direct Visualization of Wavelength-Dependent Single Dipoles Generated on Single Gold Nanourchins with Sharp Branches. *Nanoscale Research Letters*, 13(1), 256.

Kim, J., Ong, G. K., Wang, Y., et al. (2015). Nanocomposite Architecture for Rapid, Spectrally-Selective Electrochromic Modulation of Solar Transmittance. *Nano Letters*, 15(8), 5574–5579.

Lane, L. A., Qian, X., & Nie, S. (2015, October 14). SERS Nanoparticles in Medicine: From Label-Free Detection to Spectroscopic Tagging. *Chemical Reviews*. American Chemical Society.

Lapchenko, A. S. (2015). Photodynamic therapy. The fields of applications and prospects for the further development in otorhinolaryngology. *Vestnik Otorinolaringologii*. Издательство ‘Медиа Сфера’.

Le Ru, E. C., Grand, J., Sow, I., et al. (2011). A scheme for detecting every single target molecule with surface-enhanced raman spectroscopy. *Nano Letters*, 11(11), 5013–5019.

Maysinger, D., Moquin, A., Choi, J., et al. (2018). Gold nanourchins and celastrol reorganize the nucleo- and cytoskeleton of glioblastoma cells. *Nanoscale*, 10(4), 1716–1726.

Panda, S. K., Chakraborti, S., & Basu, R. N. (2018). Size and shape dependences of the colloidal silver nanoparticles on the light sources in photo-mediated citrate reduction technique. *Bulletin of Materials Science*, 41(4), 1–7.

Pastoriza-Santos, I., Pérez-Juste, J., & Liz-Marzán, L. M. (2006). Silica-Coating and Hydrophobation of CTAB-Stabilized Gold Nanorods. *Chemistry of Materials*, 18(10), 2465–2467.

Phan-Quang, G. C., Han, X., Koh, C. S. L., et al. (2019). Three-Dimensional Surface-Enhanced Raman Scattering Platforms: Large-Scale Plasmonic Hotspots for New Applications in Sensing, Microreaction, and Data Storage. *Accounts of Chemical Research*, 52(7), 1844–1854.

Ren, W., Liu, J., Guo, S., et al. (2011). SERS imaging for label-free detection of the phospholipids distribution in hybrid lipid membrane. *Science China Chemistry*, 54(8), 1334–1341.

Sahu, B. K., Dwivedi, A., Pal, K. K., et al. (2021). Optimized Au NRs for efficient SERS and SERRS performances with molecular and longitudinal surface plasmon resonance. *Applied Surface Science*, 537.

Sharma, B., Frontiera, R. R., Henry, A.-I., et al. (2012). SERS: Materials, applications, and the future. *Materials Today*, 15(1–2), 16–25.

Solovyeva, E. V., Ubyivovk, E. V., & Denisova, A. S. (2018). Effect of diaminostilbene as a molecular linker on Ag nanoparticles: SERS study of aggregation and interparticle hot spots in various environments. *Colloids and Surfaces A: Physicochemical and Engineering Aspects*, 538, 542–548.

Song, G., Lin, Y., Zhu, Z., et al. (2015). Strong Fluorescence of Poly(N-vinylpyrrolidone) and Its Oxidized Hydrolyzate. *Macromolecular Rapid Communications*, 36(3), 278–285.

Uchehara, G., Kirk, A. G., Trifiro, M., et al. (2019). Real time label-free monitoring of plasmonic polymerase chain reaction products. In Jaehwan Kim (Ed.), *Nano-, Bio-, Info-Tech Sensors and 3D Systems III* (Vol. 10969, p. 9).

Wang, K., Wang, Q., Luo, Q., et al. (2015). Fluorescence molecular tomography in the second near-infrared window. *Optics Express*, 23(10), 12669.